View Article Online / Journal Homepage / Table of Contents for this issue
Dynamic Article Links

ChemComm

Cite this: *Chem. Commun.*, 2011, **47**, 7863–7865

www.rsc.org/chemcomm

COMMUNICATION

Highly efficient photocatalytic dehalogenation of organic halides on TiO_2 loaded with bimetallic Pd–Pt alloy nanoparticles†

Yasuhiro Shiraishi,*[a] Yoshinori Takeda,[a] Yoshitsune Sugano,[a] Satoshi Ichikawa,[b] Shunsuke Tanaka[c] and Takayuki Hirai[a]

Received 12th April 2011, Accepted 17th May 2011
DOI: 10.1039/c1cc12087e

UV irradiation of TiO_2 loaded with bimetallic Pd–Pt alloy particles promotes highly efficient dehalogenation of organic halides with alcohol as a hydrogen source.

The dehalogenation of organic halides is a significant process for the removal of halogenated organic pollutants and the synthesis of fine chemicals.[1] The reaction is currently carried out *via* the hydrodehalogenation processes with catalysts containing Pd particles using molecular hydrogen (H_2) as the hydrogen source,[2] which inevitably holds explosion risks. Alternative methods with safe hydrogen sources such as alcohols are therefore desirable.

Recently, a H_2-free dehalogenation method with alcohol as the hydrogen source was proposed by Fuku *et al.*[3] They employed a photocatalytic reaction using TiO_2 loaded with 1 wt% Pd particles (Pd@TiO_2). Photoirradiation ($\lambda > 300$ nm) of a 2-PrOH solution containing chlorobenzene with Pd@TiO_2 and a base (NaOH) produces the corresponding benzene quantitatively. The reactions are initiated by photoexcitation of TiO_2, producing the electron (e^-) and positive hole (h^+) pairs (eqn (1)). The h^+ oxidizes 2-PrOH and produces acetone and protons (eqn (2)).[4] The H^+ is activated by the reduction with e^- on the Pd particles (eqn (3)), and the formed hydride species (H^-–Pd) promote dehalogenation (eqn (4)). The removed Cl^- is solidified as NaCl by the reaction with NaOH (eqn (5)). The overall reaction is expressed as eqn (6).

$$TiO_2 + h\nu \rightarrow h^+ + e^- \tag{1}$$

$$(CH_3)_2CHOH + 2h^+ \rightarrow (CH_3)_2CO + 2H^+ \tag{2}$$

$$H^+ + 2e^- + Pd \rightarrow H^-\text{–}Pd \tag{3}$$

$$Ar\text{–}Cl + H^-\text{–}Pd \rightarrow Ar\text{–}H + Cl^- + Pd \tag{4}$$

$$H^+ + Cl^- + NaOH \rightarrow H_2O + NaCl\downarrow \tag{5}$$

$$\begin{aligned} &Ar - Cl + (CH_3)_2CHOH + NaOH \\ &\xrightarrow{h\nu,TiO_2} Ar - H + (CH_3)_2CO + H_2O + NaCl\downarrow \end{aligned} \tag{6}$$

These reactions proceed at room temperature with alcohol as the hydrogen source, and have a potential to be a safe and sustainable dehalogenation process. The reactions, however, proceed very slowly when compared to the conventional method with H_2. The activity improvement is therefore necessary.

Herein, we report that TiO_2 loaded with bimetallic Pd–Pt alloy particles (PdPt@TiO_2) promotes highly efficient photocatalytic dehalogenation. The activity is more than three times that of Pd@TiO_2 and higher than the conventional method with H_2. The high activity is due to the enhanced consumption of photoformed e^- on the Pt site by H^+ reduction and efficient transfer of the formed hydrogen atom to the adjacent Pd site within the alloy particles.

Pd_1Pt_y@TiO_2 with Pd–Pt alloy consisting of 1 wt% Pd [$=Pd/TiO_2 \times 100$] and different amounts of Pt [y (wt%) $= Pt/TiO_2 \times 100$] were prepared with Japan Reference Catalyst JRC-TIO-4 TiO_2 (equivalent to Degussa P25) by simultaneous impregnation of $Pd(NO_3)_2$ and H_2PtCl_6 followed by reduction with H_2 (see ESI†).[5] A transmission electron microscopy (TEM) image of Pd_1Pt_5@TiO_2 showed spherical metal particles with an average diameter of 2.9 nm (Fig. 1). The lower or higher Pt loadings create smaller or larger particles; Pd_1Pt_1 and Pd_1Pt_{10} contain 2.5 and 3.4 nm particles, respectively (Fig. S1, ESI†). An X-ray photoelectron spectroscopy (XPS) of catalysts confirmed the presence of both Pd and Pt (Fig. S2, ESI†). An energy dispersive X-ray spectroscopy (EDX) of metal particles on Pd_1Pt_5@TiO_2 (Fig. S3, ESI†) determined the average Pt/Pd ratio as 4.95 (wt/wt), which is close to the ratio of the total amount of Pt and Pd (4.96) determined by ICP analysis. An X-ray diffraction (XRD) pattern of Pd_1Pt_5@TiO_2 (Fig. S4, ESI†) shows a (111) diffraction of the Pd–Pt alloy at 39.9°, which is located between the Pt(111) and Pd(111) diffractions (39.8° and 40.2°). The lattice parameter of the alloy calculated from the XRD data (a = 0.391 nm) agrees with that calculated with the Vegard's law[6] (0.391 nm). In addition, the d-value calculated from the lattice spacing of the alloy in the TEM image (d_{111} = 0.225 nm, Fig. S5, ESI†) is in between the standard Pt (d_{111} = 0.2265 nm, JCPDS 04-0802)

---

[a] *Research Center for Solar Energy Chemistry, and Division of Chemical Engineering, Graduate School of Engineering Science, Osaka University, Toyonaka, 560-8531, Japan. E-mail: shiraish@cheng.es.osaka-u.ac.jp; Fax: +81-6-6850-6273; Tel: +81-6-6850-6271*
[b] *Institute for NanoScience Design Center, Osaka University, Toyonaka 560-8531, Japan*
[c] *Department of Chemical, Energy and Environmental Engineering, Kansai University, Suita 564-8680, Japan*

† Electronic supplementary information (ESI) available: Methods and data (Fig. S1–S7 and Table 1). See DOI: 10.1039/c1cc12087e

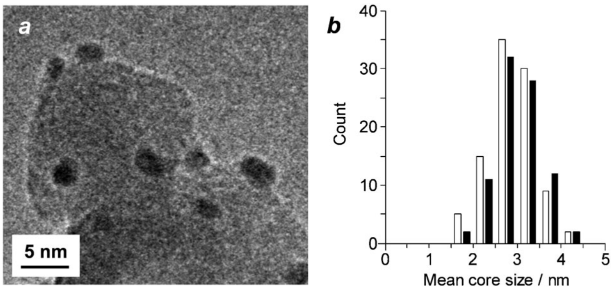

Fig. 1 (a) TEM image of $Pd_1Pt_5@TiO_2$ and (b) size distribution of metal particles on (white) the fresh catalyst and (black) the catalyst recovered after 2nd reuse in reaction (Table 1, run 16).

and Pd (d_{111} = 0.2246 nm, JCPDS 46-1043). These indicate that Pd–Pt alloy particles are indeed loaded on TiO_2. Diffuse reflectance UV-vis spectra (Fig. S6, ESI†) revealed that $Pd_1Pt_y@TiO_2$ with higher Pt loadings show increased absorbance at >300 nm due to light scattering by the Pt particles.

Table 1 summarizes the results of photocatalytic reaction ($\lambda > 300$ nm) of *p*-chlorotoluene (0.2 mmol) in 2-PrOH (5 mL) with catalysts (5 mg) and NaOH (0.5 mmol) for 1 h at 298 K under Ar. The results obtained using H_2 (1 atm) in the dark at 298 K are also shown for comparison. Both photocatalytic and H_2 systems (runs 1–9) selectively produce toluene. The toluene yields in the photocatalytic system with the catalysts containing Pd alone, $Pd_x@TiO_2$ [x (wt%) = Pd/TiO_2 × 100], are less than 21% (runs 1–4). In contrast, the yields in the H_2 system with $Pd_x@TiO_2$ are *ca.* 50%, indicating that the photocatalytic system is indeed inefficient.

The loading of Pd–Pt alloy particles significantly enhances the photocatalytic dechlorination (runs 5–9): $Pd_1Pt_y@TiO_2$ show increased toluene yields with an increase in the Pt amount of the particles, where $Pd_1Pt_5@TiO_2$ shows the highest yield (76%), which is more than three times that of $Pd_x@TiO_2$. In contrast, such alloying effect is not observed in the H_2 system (runs 5–9); the toluene yields decrease monotonically with the Pt loadings ($<56\%$).

It is noted that the catalysts containing Pt alone, $Pt_y@TiO_2$ [y (wt%) = Pt/TiO_2 × 100], do not promote dechlorination (runs 10–13). This indicates that, on the alloy catalysts, the Pd site is active for dehalogenation. It is also noted that the Pd–Pt alloy site is necessary for efficient dehalogenation: a Pd_1 + $Pt_5@TiO_2$ catalyst (run 14), prepared by a step-by-step deposition of respective Pd and Pt particles (see ESI†), scarcely enhances dehalogenation.

The high activity of the alloy catalyst is due to the efficient consumption of photoformed e^- by H^+ reduction on the Pt site and efficient transfer of the formed H atom to the adjacent Pd site (Scheme 1a). The efficient e^- consumption on Pt is confirmed by the amount of formed acetone (Table 1). $Pd_x@TiO_2$ produce <45 μmol acetone (runs 1–4), whereas $Pt_y@TiO_2$ produce larger amounts (runs 10–13). This is because e^- is efficiently trapped by Pt due to the larger work function[7] and consumed by H^+ reduction, facilitating efficient alcohol oxidation by h^+. As shown in run 12, $Pt_5@TiO_2$ produces the largest amount of acetone among $Pt_y@TiO_2$ and higher Pt loadings decrease the production. A similar tendency is observed for $Pd_1Pt_y@TiO_2$: Pd_1Pt_5 produces the largest amount of acetone. The higher activity of $Pd_1Pt_5@TiO_2$ than $Pd@TiO_2$ is thus because the photoformed e^- is efficiently consumed by H^+ reduction on the Pt site, producing a H atom.[8]

$$H^+ + e^- + Pt \rightarrow H\text{–}Pt \qquad (7)$$

The H atom on Pt within the alloy particles is efficiently used for dehalogenation. This is confirmed by the H^+ balance, defined as the ratio of the formed dehalogenation product to that of the formed H^+. As shown by eqn (6), two H^+ formed

Table 1 Results of dechlorination of *p*-chlorotoluene in the photocatalytic and H_2 systems[a]

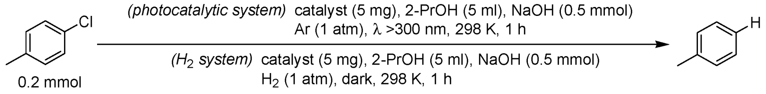

			Photocatalytic system				H_2 system	
Run	Catalyst	Metal particle size[b]/nm	*p*-Chlorotoluene conv. (%)	Toluene yield (%)	Acetone formed/μmol	H^+ balance[c]	*p*-Chlorotoluene conv. (%)	Toluene yield (%)
1	$Pd_1@TiO_2$	5.3	20	19	42	0.92	56	54
2	$Pd_3@TiO_2$		21	20	43	0.96	56	54
3	$Pd_5@TiO_2$		19	18	41	0.88	52	51
4	$Pd_7@TiO_2$		14	13	29	0.90	35	34
5	$Pd_1Pt_1@TiO_2$	2.5	28	27	55	0.97	32	31
6	$Pd_1Pt_3@TiO_2$		45	43	88	0.97	26	23
7	$Pd_1Pt_5@TiO_2$	2.9	76	76	155	0.98	21	20
8	$Pd_1Pt_7@TiO_2$		39	38	80	0.95	15	13
9	$Pd_1Pt_{10}@TiO_2$	3.4	36	35	79	0.90	12	11
10	$Pt_1@TiO_2$	2.2	0	0	43		0	0
11	$Pt_3@TiO_2$		0	0	65		0	0
12	$Pt_5@TiO_2$	3.9	0	0	102		0	0
13	$Pt_7@TiO_2$		0	0	79		0	0
14	Pd_1 + $Pt_5@TiO_2$		27	26	118	0.44	26	25
15[d]	$Pd_1Pt_5@TiO_2$		75	75				
16[e]	$Pd_1Pt_5@TiO_2$	3.1[f]	75	75				

[a] The results obtained with $Pd_1Pt_5@TiO_2$ in other solvents are summarized in Table S1 (ESI†). [b] TEM micrographs and the size distributions are shown in Fig. S1 (ESI†). [c] Determined by eqn (8). [d] 1st reuse after washing with 2-PrOH. [e] 2nd reuse. [f] Measured after 2nd reuse.

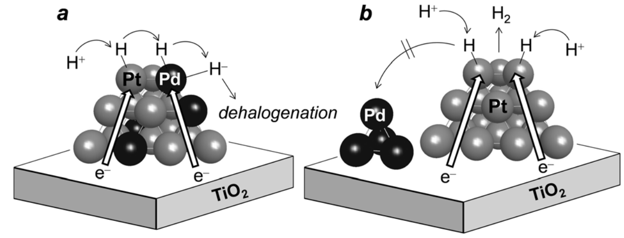

Scheme 1 The reaction sequence for protons on the metal particles of (a) $Pd_1Pt_5@TiO_2$ and (b) Pd_1 + $Pt_5@TiO_2$ catalysts.

by photooxidation of 2-PrOH are consumed by dehalogenation (eqn (3) and (4)) and reaction with NaOH (eqn (5)), respectively. The H^+ balance is therefore expressed by the ratio of the amount of formed toluene to that of formed acetone,

$$H^+ \text{ balance} = [\text{toluene formed}]/[\text{acetone formed}] \qquad (8)$$

Table 1 summarizes the H^+ balance for the respective systems obtained by photoreaction for 1 h. The values for $Pd_x@TiO_2$ are almost 1 (runs 1–4), indicating that H^+ formed by alcohol oxidation are consumed quantitatively by dehalogenation on Pd (eqn (6)).[3] The values for $PdPt@TiO_2$ are also almost 1 (runs 5–9), suggesting that H^+ are also consumed quantitatively although H^+ are reduced on Pt (eqn (7)). The results suggest that, as shown in Scheme 1a, the H atom formed on Pt is transferred to the adjacent Pd site (H–Pd formation), which is probably due to the stronger H–Pd interaction.[9]

$$\text{H–Pt} \rightarrow \text{H–Pd} \qquad (9)$$

The H atom is reduced to the hydride species (H^-–Pd) by e^-, which promotes dechlorination (eqn (4)).

$$\text{H–Pd} + e^- \rightarrow H^-\text{–Pd} \qquad (10)$$

As shown in run 14, the H^+ balance for the Pd_1 + $Pt_5@TiO_2$ system is only 0.44. This is because the absence of Pd around the Pt site suppresses the H transfer from Pt to Pd and results in removal of H atoms by H_2 formation (Scheme 1b).[10]

$$\text{H–Pt} + \text{H–Pt} \rightarrow H_2\uparrow + 2\text{Pt} \qquad (11)$$

Change in H_2 amount during reaction confirms this (Fig. S7, ESI†). Pd_1 + $Pt_5@TiO_2$ promotes H_2 formation and dechlorination simultaneously; however, $Pd_1Pt_5@TiO_2$ scarcely produces H_2 until *p*-chlorotoluene disappears. The alloy sites are therefore necessary for efficient H transfer from the Pt to Pd sites.

The above results reveal that, on the alloy site (Scheme 1a), efficient reduction of H^+ by e^- on Pt, smooth H transfer to Pd, and reduction of H by e^- occur sequentially. This sequence produces a large amount of H^-–Pd species and promotes efficient dehalogenation. It must be noted that, as shown in runs 15 and 16 (Table 1), the alloy catalyst is reusable for dehalogenation at least two times without loss of activity and selectivity. In addition, as shown in Fig. 1b, the size of Pd–Pt alloy particles scarcely changes even after the reaction.

The alloy catalyst is tolerant for photocatalytic dehalogenation of various aromatic halides (Table 2). $Pd_1Pt_5@TiO_2$ produces the corresponding dehalogenation compounds with very high yield, and the catalytic activities are much higher than those obtained with $Pd_1@TiO_2$ using H_2.

Table 2 Dehalogenation of various aromatic halides

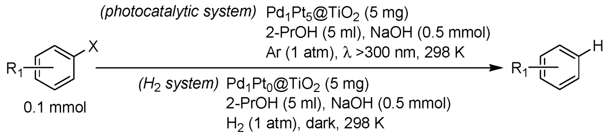

Run	Substrate	System	Time/h	Conv. (%)	Yield (%)
1	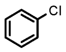	Photo	1.5	99	97
2		H_2	1.5	74	72
3	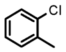	Photo	1	>99	99
4		H_2	1	52	51
5	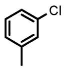	Photo	1	>99	99
6		H_2	1	58	57
7	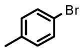	Photo	1	>99	99
8		H_2	1	77	76
9	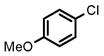	Photo	1	>99	97
10		H_2	1	76	75
11	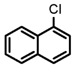	Photo	2	97	96
12		H_2	2	51	49
13	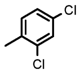	Photo	2	92	87 (toluene)
14		H_2	2	60	37 (toluene)

In summary, we found that UV irradiation of TiO_2 loaded with Pd–Pt alloy promotes efficient dehalogenation. This offers crucial advantages: (i) safe alcohols can be used as a hydrogen source; and, (ii) the reaction proceeds much faster. The alloy catalyst that facilitates efficient production of active species (H^-–Pd) may also promote other hydrogenation reactions, and the work along these lines is currently in progress.

This work was supported by a Grant-in-Aid for Scientific Research (No. 23360349) from the Ministry of Education, Culture, Sports, Science and Technology, Japan (MEXT).

Notes and references

1 (*a*) F. Alonso, I. P. Beletskaya and M. Yus, *Chem. Rev.*, 2002, **102**, 4009; (*b*) V. V. Grushin and H. Alper, *Chem. Rev.*, 1994, **94**, 1047; (*c*) A. R. Pinder, *Synthesis*, 1980, 425; (*d*) M. L. Hitchman, R. A. Spackman and C. Agra, *Chem. Soc. Rev.*, 1995, **95**, 423.
2 (*a*) K. Kaneda, T. Hara, T. Kaneta, K. Mori, T. Mitsudome, T. Mizugaki and K. Ebitani, *Green Chem.*, 2007, **9**, 1246; (*b*) R. B. Lapierre, L. Guczi, W. L. Kranich and A. H. Weiss, *J. Catal.*, 1978, **52**, 230; (*c*) G. Yuan and M. A. Keane, *Ind. Eng. Chem. Res.*, 2007, **46**, 705.
3 K. Fuku, K. Hashimoto and H. Kominami, *Chem. Commun.*, 2010, **46**, 5118.
4 Y. Shiraishi, Y. Sugano, S. Tanaka and T. Hirai, *Angew. Chem., Int. Ed.*, 2010, **49**, 1656.
5 M. Legawiec-Jarzyna, A. Srebowata, W. Juszczyk and Z. Karpinski, *Catal. Today*, 2004, **88**, 93.
6 L. Vegard, *Z. Phys.*, 1921, **5**, 17.
7 B. Herbert and J. Michaelson, *J. Appl. Phys.*, 1977, **48**, 4728.
8 (*a*) Y. Z. Yang, C.-H. Chang and H. Idriss, *Appl. Catal., B*, 2006, **67**, 217; (*b*) N. Strataki, M. Antoniadou, V. Dracopoulos and P. Lianos, *Catal. Today*, 2010, **151**, 53.
9 M. Yamauchi, H. Kobayashi and H. Kitagawa, *ChemPhysChem*, 2009, **10**, 2566.
10 B. Ohtani, K. Iwai, S. Nishimoto and S. Sato, *J. Phys. Chem. B*, 1997, **101**, 3349.